

Ex vivo culturing of stromal cells with dexamethasone-loaded carboxymethylchitosan/poly(amidoamine) dendrimer nanoparticles promotes ectopic bone formation

J.M. Oliveira ^{a,b,c}, N. Kotobuki ^c, M. Tadokoro ^c, M. Hirose ^c, J.F. Mano ^{a,b}, R.L. Reis ^{a,b,*}, H. Ohgushi ^c

^a 3B's Research Group - Biomaterials, Biodegradables and Biomimetics, Univ. Minho, Headquarters of the European Institute of Excellence on Tissue Engineering and Regenerative Medicine, AvePark, S. Cláudio de Barco, 4806-909 Taipas, Guimarães, Portugal

^b IBB - Institute for Biotechnology and Bioengineering, PT Government Associated Laboratory, Guimarães, Portugal

^c Research Institute for Cell Engineering (RICE), National Institute of Advanced Industrial Science and Technology (AIST), Nakoji 3-11-46, Amagasaki, 661-0974 Hyogo, Japan

ARTICLE INFO

Article history:

Received 17 December 2009

Revised 19 January 2010

Accepted 3 February 2010

Available online 10 February 2010

Edited by: D. Burr

Keywords:

Bone histomorphometry

Bone marrow stromal cells

Dexamethasone-loaded

carboxymethylchitosan/poly(amidoamine)

dendrimer nanoparticles

Hydroxyapatite

In vivo test

ABSTRACT

Recently, our group has proposed a combinatorial strategy in tissue engineering principles employing carboxymethylchitosan/poly(amidoamine) dendrimer nanoparticles (CMCh/PAMAM) towards the intracellular release and regimented supply of dexamethasone (Dex) aimed at controlling stem cell osteogenic differentiation in the absence of typical osteogenic inducers, *in vivo*. In this work, we have investigated if the Dex-loaded CMCh/PAMAM dendrimer nanoparticles could play a crucial role in the regulation of osteogenesis, *in vivo*. Macroporous hydroxyapatite (HA) scaffolds were seeded with rat bone marrow stromal cells (RBMSCs), whose cells were expanded in MEM medium supplemented with 0.01 mg ml⁻¹ Dex-loaded CMCh/PAMAM dendrimer nanoparticles and implanted subcutaneously on the back of rats for 2 and 4 weeks. HA porous ceramics without RBMSCs and RBMSCs/HA scaffold constructs seeded with cells expanded in the presence and absence of 10⁻⁸ M Dex were used as controls. The effect of initial cell number seeded in the HA scaffolds on the bone-forming ability of the constructs was also investigated. Qualitative and quantitative new bone formation was evaluated in a non-destructive manner using micro-computed tomography analyses of the explants. Haematoxylin and Eosin stained implant sections were also used for the histomorphometrical analysis. Toluidine blue staining was carried out to investigate the synthesis of proteoglycan extracellular matrix. In addition, alkaline phosphatase and osteocalcin levels in the explants were also quantified, since these markers denote osteogenic differentiation. At 4 weeks post-implantation results have shown that the novel Dex-loaded carboxymethylchitosan/poly(amidoamine) dendrimer nanoparticles may be beneficial as an intracellular nanocarrier, supplying Dex in a regimented manner and promoting superior ectopic *de novo* bone formation.

© 2010 Elsevier Inc. All rights reserved.

Introduction

A variety of hydroxyapatite (HA) ceramics with controlled architectures [1–3] has been developed to find applications as bone substitutes in the clinic. Despite, their interesting architecture namely pore size, shape and interconnectivity, mechanical properties and important biological role in the *in vivo* performance, these porous implants lack on its osteoinductive capacity [4–6]. In this regard, it has been shown that porous HA ceramics alone, do not induce bone formation in soft tissues when implanted in rabbits [7], or upon subcutaneous implantation in mice [8,9], rats [10–12] and goats [13].

By its turn, bone marrow stromal cells (BMSCs) have shown to inherently possess a huge therapeutic potential [14–20]. As a possible alternative, a combination of bone marrow stromal cells (BMSCs) with porous scaffolds [10,11,13,21] has been widely explored in bone tissue engineering strategies. On the other hand, it has been shown that glucocorticoids such as dexamethasone (Dex) have an essential role for osteoblast differentiation and matrix mineralization [22–24]. In fact, it has been reported that Dex regulation depends on the degree of cellular differentiation, the donor species, and dosage, dose duration and dosing regimen [25]. Several authors [9,10,26] reported that stem cells need to be under the influence of such type of osteogenic factors for superior *de novo* bone formation. Actually, cell-scaffold constructs showed *in vivo* bone formation within the pores of the scaffolds when constructs were firstly *in vitro* cultured under osteogenic factors [10,11]. However, the long culturing time is a major drawback of this strategy and may not be the most feasible to satisfactorily meet clinical demands. Bearing in mind these premises,

* Corresponding author. 3B's Research Group - Biomaterials, Biodegradables and Biomimetics, Univ. Minho, Headquarters of the European Institute of Excellence on Tissue Engineering and Regenerative Medicine, AvePark, S. Cláudio de Barco, 4806-909 Taipas, Guimarães, Portugal. Fax: +351 253510909.

E-mail address: rgreis@dep.uminho.pt (R.L. Reis).

we foresee that cells may not maintain *in vivo* the cellular phenotype upon withdrawal of Dex, since Dex acts at both early and late stages to direct proliferative osteoprogenitor cells toward terminal maturation [27]. In fact, Castano-Izquierdo et al. [28] demonstrated that an *in vitro* pre-culture period of rat mesenchymal stem cells (rMSCs) in osteogenic media influences their *in vivo* bone-forming potential when implanted to an orthotopic site (rat critical cranial size defect). This study revealed that an enhanced *de novo* bone formation occurred when *in vitro* pre-culture of rMSCs lasted for 4 days, while the lowest bone formation was obtained with rMSCs cultured for 16 days. Therefore, the role of Dex is a critical factor in bone tissue regeneration and still remains an open issue [29] that needs further research namely what concerns with the development of alternative approaches to improve the limited cell-derived osteogenesis. In this context, we have been hypothesizing that the *ex vivo* culturing of stem cells with functional nanoparticles which can be efficiently taken up by cells may influence their cellular fate in the absence of typical osteogenic inducers, *in vivo*. It has been shown that glucocorticoids such as Dex bind to and triggers the cytoplasmatic glucocorticoid receptor [30,31]. Thus, we expect that the culturing of stem cells in the presence of nanoparticles that release Dex from inside, and in a regimented manner may be an effective strategy for *in vivo* control of stem cell osteogenic differentiation and maturation. In this regard, we have surface engineered low generation poly(amidoamine) dendrimers with carboxymethylchitosan, CMCh/PAMAM dendrimer nanoparticles and loaded them with Dex [32]. These are expected to possess high drug loading ability and non-cytotoxic behaviour as compared to amine-terminated poly(amidoamine) dendrimers of high generation. The use of Dex-loaded CMCh/PAMAM dendrimer nanoparticles can also allow to avoid the need and frequency of drug administration as Dex which is available at the target site possibly minimizes the undesired side effects [31].

In previous studies [32,33], we have shown the high efficiency of Dex-loaded CMCh/PAMAM dendrimer nanoparticles on being internalized by different cell types, *in vitro*. The Dex release profile from the CMCh/PAMAM nanoparticles was monitored, in the presence and absence of serum proteins at physiological pH. This study has shown that Dex is released as a free drug in the range of concentrations similar to that of typical osteogenic cocktails. Complementarily, we demonstrated their role in promoting the osteogenic differentiation of rat bone marrow stromal cells (RBMSCs) in tissue culture polystyrene, TCPS dishes.

Our group [34,35] has recently developed HA scaffolds with macroporous structure and reported that they are non-cytotoxic and efficiently support the adhesion, proliferation and osteogenic differentiation of RBMSCs in the presence of 0.01 mg ml^{-1} Dex-loaded CMCh/PAMAM dendrimer nanoparticles, *in vitro*. Thus, the HA scaffolds have shown to possess promising physicochemical and biological properties for use in bone tissue engineering approaches. To further evaluate the *in vivo* performance of the cell-scaffold constructs, several groups [10,11,26,36] have been proposing the well established ectopic implantation model in rats. This is a cost effective model [37] and allows to avoid the presence of growth factors found at the orthotopic site whose influence may affect the performance of the constructs [38].

In the current experimental study, we investigate if the Dex-loaded CMCh/PAMAM dendrimer nanoparticles play a crucial role in the regulation of osteogenesis, *in vivo*. We therefore used RBMSCs/HA construct whose cells were exposed to 0.01 mg ml^{-1} Dex-loaded CMCh/PAMAM dendrimer nanoparticles during the expansion time (Fig. 1, top) and assess their efficiency in promoting the osteogenic differentiation and *de novo* bone formation upon subcutaneous implantation on the back of rats for the period of 2 and 4 weeks. HA macroporous ceramics and RBMSCs/HA constructs seeded with different cell numbers and cultured either in the presence or absence of Dex were used as controls for elucidating the role of the Dex-loaded

CMCh/PAMAM dendrimer nanoparticles in promoting osteogenesis. Micro-computed tomography (micro-CT) analyses were performed to investigate new bone formation in the RBMSCs/HA constructs. Histological studies were also carried out using Haematoxylin and Eosin staining. Histomorphometrical analysis of the implant sections and 3D micro-CT reconstructions were performed to quantify new bone formation. Toluidine blue staining was also performed to investigate the synthesis of proteoglycan extracellular matrix. Complementarily, osteoblastic phenotype expression levels were determined by quantification of the surface-membrane alkaline phosphatase (ALP) glycoprotein and osteocalcin, the early and late markers of osteogenic differentiation, respectively [39,40].

Materials and methods

Preparation of the hydroxyapatite (HA) scaffolds and synthesis of dexamethasone-loaded carboxymethylchitosan/poly(amidoamine) dendrimer (Dex-loaded CMCh/PAMAM dendrimer nanoparticles)

Sintered HA scaffolds with 5 mm diameter and 4 mm height were obtained by means of impregnating a polyurethane (PU, Eurospuma S.A., Portugal) sponge with HA powders, as previously reported [34,41,42]. The porosity of the HA scaffolds was evaluated by means of micro-computed tomography (μ -CT) analysis (Scanco Medicals, Switzerland) and using the Mimics[®] image processing software (Materialise, Belgium). Standardized fabrication conditions enabled the production of HA scaffolds with a pore size ranging from 50 to 600 μm , and a mean porosity of $67.8 \pm 5.0\%$. Further details on the HA scaffolds can be found elsewhere [34].

Carboxymethylchitosan (CMCh) was synthesized by a chemical modification route of chitin (Sigma, Germany) as described by Chen et al. [43]. Starburst[®] poly(amidoamine)-carboxylic-terminated dendrimers, PAMAM-CT (generation 1.5, 20% (w/v) methanolic solution) with an ethylenediamine core were purchased from Aldrich (Germany). Dexamethasone-loaded carboxymethylchitosan/poly(amidoamine) dendrimer nanoparticles (Dex-loaded CMCh/PAMAM) were prepared in a stepwise manner as previously described [32]. In brief, CMCh/PAMAM dendrimer nanoparticles were prepared by dissolving appropriate amounts of a firstly synthesized PAMAM-ester terminated dendrimer and CMCh in a water/methanol solution (condensation reaction). CMCh/PAMAM dendrimer nanoparticles with carboxylic-terminated groups were obtained by reductive *N*-alkylation. Dexamethasone (Dex, Sigma, Germany) with a final concentration of $5 \times 10^{-4} \text{ M}$ was added to the dendrimer solution. The precipitation of nanoparticles was carried out by adding a saturated sodium carbonate (Aldrich, Germany) solution. Then, Dex-loaded CMCh/PAMAM dendrimer nanoparticles were collected by filtration, dissolved in ultrapure water and dialyzed using a dialysis tubing benzoylated (Sigma, Germany) for 2 days. Finally, the nanoparticles solution was frozen at -80°C and lyophilized (Telstar-Cryodos –80, Spain).

Prior to the *in vitro* cell culture the HA scaffolds and Dex-loaded CMCh/PAMAM dendrimer nanoparticles were sterilized under an ethylene oxide (EtOx) gas atmosphere. No deleterious effect on physicochemical properties and cytotoxic behaviour of these materials [32,34,35] have been observed after EtOx sterilization.

In vitro cell culture

Isolation and expansion of rat bone marrow stromal cells (RBMSCs)

Seven-week-old Fischer 344/N male rats (Japan SLC Inc., Shizuoka, Japan) were sacrificed by administrating an excess of anesthesia, in accordance to the Ethics Committee at the Tissue Engineering Research Center (Amagasaki, Japan). The marrow plugs in the femoral shafts were flush out using Eagle's minimum essential medium (MEM, Nacalai Tesque, Japan) supplemented with 15% fetal bovine serum

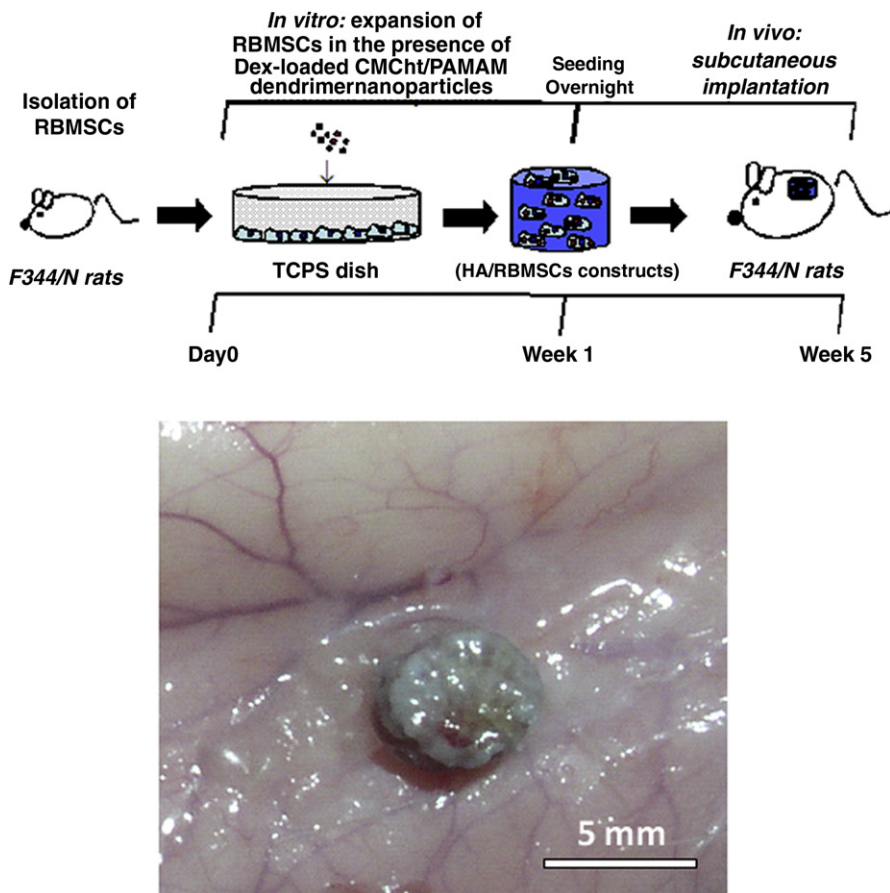


Fig. 1. Schematic representation of the experimental strategy (top) and photo of the RBMSCs/HA explants with RBMSCs expanded in MEM medium supplemented with 0.01 mg ml^{-1} Dex-loaded CMCh/PAMAM dendrimer nanoparticles, after 4 weeks of subcutaneous implantation (bottom).

(FBS, JRH Biosciences, USA) and 1% antibiotic–antimycotic (A/B, Nacalai Tesque, Japan) solution, as described elsewhere [44]. RBMSCs were transferred to T75 cm² culture flask and cultured in the presence of different culture media for the period of 1 week: complete MEM medium, MEM medium supplemented with 0.01 mg ml^{-1} Dex-loaded CMCh/PAMAM dendrimer nanoparticles and MEM medium supplemented with 10^{-8} M Dex at 37 °C in a 5% CO₂ incubator. The culture medium was changed within 3 days to remove non-adherent cells. Then, the culture medium was changed every 2 or 3 days.

Seeding of RBMSCs onto the surface of the HA scaffolds

The RBMSCs (passage 1, P1) were released from substratum with 1 ml of 0.05% trypsin–0.53 mM EDTA (Invitrogen, USA) and centrifuged at 900 rpm for 5 min, after culturing for 1 week. The supernatant was aspirated and the cells re-suspended with 10 ml of complete culture medium. Cell concentration was determined using an automatic cell counter (Cell Counter Sysmex F-520, Japan). Prior to seeding, the viability of the RBMSCs was also analyzed with a NucleoCounter (ChemoMetec A/S, Denmark) [45]. In addition, the HA scaffolds were de-aired in MEM medium under vacuum and following the protocol described elsewhere [35]. Succinctly, the air was removed from the porous materials by setting the following apparatus: five scaffolds were placed in a 13 ml tube with polystyrene ventilation cap containing 3 ml of culture medium. A 21 G needle was attached to a 20 ml syringe and the needle was inserted through the cap of the tube. By pulling the plunger back completely, a partial vacuum was created in the tube. Then, negative pressure was kept for 5–10 min until no bubbling was observed. Finally, one scaffold was placed in a well of a 96-well TCPS plate and RBMSCs were seeded in a drop-wise manner, and in static conditions. RBMSCs expanded in a

complete MEM medium, MEM medium supplemented with 0.01 mg ml^{-1} Dex-loaded CMCh/PAMAM dendrimer nanoparticles and MEM medium supplemented with 10^{-8} M Dex were seeded onto each HA scaffold. The effect of cell density was evaluated by seeding different cell numbers (1×10^6 and 2×10^5) onto the HA scaffolds. Finally, RBMSCs/HA scaffold constructs were cultured in the complete MEM medium for the period of 12 h to allow cell adhesion, under standard culture conditions.

In vivo study

Subcutaneous implantation

Seven-week-old male Fischer 344 rat (Syngeneic F344/N rat), same as donor sub-strain and age, were anesthetized by intraperitoneal injection of pentobarbital (Nembutal, Dainippon Pharmaceutical Co. Ltd., Japan) at a final concentration of 3.5 mg per 100 g of body weight. The hair of the rat was cut at the implantation area, followed by washing with tap water and scrubbed with tincture of iodine and 70% ethanol. In each rat, three or four skin incisions (each 1 cm length) on the dorsal midline below the ear were made. Each RBMSCs/HA construct was implanted subcutaneously (1.5 to 2 cm away from the midline at both right and left sides) into the respective pocket and skin sutured. As a negative control, we used HA implants without RBMSCs. A maximum of 8 RBMSCs/HA constructs were implanted per F344/N rat and no prophylactic medication was administered post-surgery.

After 2 and 4 weeks of implantation, the animals were sacrificed with an overdose of anesthetic and the implants were retrieved. The *in vivo* implantation time was chosen based on our preliminary animal testing and on previous work reported by Ohgushi group [44,45]. All

in vivo experiments were carried out 3 times and using a minimum of three implants per condition.

Micro-computed tomography (micro-CT) analyses

New bone formation in the retrieved implants was investigated by micro-computed tomography (micro-CT: MCT-CB 100MF(Z); Hitachi Medical Corp., Tokyo, Japan) analyses. After 2 and 4 weeks of implantation, implants were retrieved, rinsed with PBS, and fixed with 10% formalin at room temperature, overnight. Constructs were placed on a flat surface for analysis under the micro-CT. X-ray scans were acquired with a resolution mode of 10 µm (x/y/z) at 50 kV and 150 µA. The analytical conditions were: precision mode, and 7 times magnification with an image intensifier field of 4.57 cm [46]. Three explants per condition were analyzed using the 3D Bone Morphometry (TRI/3D-Bon, RATOC System Engineering Co. Ltd., Tokyo, Japan) software for evaluate the 2D distribution of newly formed bone within the pores of the explants.

The 3D bone formation within the HA implants was quantified using the Mimics® image processing software (Materialise, Belgium). The bone volume (mm³) formed within the explants was quantified by setting the following conditions: contrast (1001–4080) and a threshold (1728–2287). A total of 256 slices per each explant were analyzed. The threshold used to quantify the new bone formed was within the range of the predefined threshold set for compact bone in adult (1686–3012).

Histological evaluation of the explants

After micro-CT analyses, explants were decalcified with K-CX solution (Falma Co., Tokyo, Japan) for histological analysis. Firstly, the constructs were dehydrated in an ascending series grade ethanol/water solution (from 90 to 100%) using an automatic machine for 19 h followed by washing three times with xylene. Then, specimens were immersed in paraffin at 62 °C and allowed to solidify at –5 °C. Slides were prepared by cutting the specimens into sections 5 µm thick using a microtome, and mounted in a micro-slide glass (Matsunami glass Ind. Ltd., Japan). Paraffin was melted by placing the slides in the oven at 71 °C for 20 min and allowed to cool down at a room temperature. The remnant paraffin was then eliminated off in hexane for 5 min (S.T. Chemical, Japan), followed by dipping into an ethylene/propylene mixture (Clear Plus, Falma Co., Tokyo, Japan) for 3 min. Then, slides were immersed three times in 100% ethanol for 2 min each time of immersion. A total of 3 explants per condition were prepared for histology.

For the Haematoxylin and Eosin (H&E) staining, slides were sequentially transferred to a 90% ethanol and then to a 70% ethanol solution and washed with tap water. It followed the staining step, which consisted of the immersion of the slides into the GM's Haematoxylin dye (Muto Pure Chemicals Co. Ltd, Tokyo, Japan, GM Haematoxylin Staining for H&E staining no. 3008-1) for 10 min. It followed the washing step with tap water for 5 to 10 min. Then, slides were rinsed with de-ionized water and immersed in a 70% ethanol solution. Finally, slides were immersed in Eosin dye (Muto Pure Chemicals Co. Ltd, Tokyo, Japan no. 3204-2) solution for 2 min and dehydrated in a series of ethanol grades (70%, 90%, and 100%). At last they were immersed three times in an ethylene/propylene mixture and then mounted to avoid the formation of bubbles for observation.

For Toluidine blue staining, paraffin was melted and slides were rinsed with ultrapure water. The ground sections were stained with 0.05% Toluidine blue (Muto Pure Chemicals Co. Ltd., Tokyo, Japan) for 30 min. Finally, the slides were dehydrated in a series of ethanol grades (70%, 90%, and 100%) and mounted for further observation. All slides were examined under a light microscope (Olympus DP70, Olympus Co. Ltd, Japan). 2D histological sections are given for the same bone specimens used in the micro-CT analyses.

Histomorphometry

Bone histomorphometry was carried out using the public domain image processing program IMAGE J (National Institutes of Health, Bethesda, MD). The light microscopy photographs of the 2D histological decalcified sections of each sample were converted to gray-value images and several filter steps were performed [47]. Shrinkage percentage observed in decalcified sections [46] was not considered in the calculations. New bone formation (NB) was expressed as a percentage of bone volume density (BV/TSV, bone volume/tissue plus scaffold volume) ± standard deviation. A minimum of 12 sections per explant were analyzed.

Quantification of alkaline phosphatase (ALP)

Alkaline phosphatase was measured to evaluate osteoblast differentiation. Prior to the assay, the explants were washed with Ca and Mg-free PBS solution. Then, explants were transferred to a 2 ml Eppendorf and pulverized with zirconia's balls as previously reported [35]. Prior to analysis the samples were sonicated and centrifuged at 12,000 rpm for 1 min at 4 °C. A minimum of 3 explants per condition were used and experiments were carried out 3 times. To each well of a 96-well plate was added an aliquot of supernatant and p-nytrophenyl phosphate substrate (ZYMED® Laboratories, Invitrogen, USA). The plate was then incubated in the dark for 30 min at 37 °C and after that time the reaction was stopped with 1 M NaOH (Panreac, Japan). Standards were prepared with p-nytrophenol, pNP. Triplicates were made for each sample and standard. Absorbance was read at 405 nm (Wallac ARVOsx 1420, Perkin-Elmer Life and Analytical Sciences, USA), and sample concentrations were read off from the standard graph. Enzyme activity was expressed either as nmol of pNP released/explant/30 min.

Quantification of osteocalcin

The remnant of each sample used for the ALP assay was treated with a 20% formic acid solution and stored at 4 °C for 2–3 days. Afterwards samples were centrifuged at 15,000 rpm for 10 min at 4 °C. Then, the supernatant was passed through a Sephadex™ G-25 column (GE healthcare, Sweden), subsequently concentrated for performing the enzyme-linked immunosorbent assay (ELISA). A Rat Osteocalcin EIA kit (no. BT-460, Biomedical Technologies Inc., MA, USA) was used following the instructions provided by the supplier. Data was read off from the standard curve obtained with human osteocalcin and expressed as ng of deposited osteocalcin per explant.

Statistical analysis

One-way analysis of variance (Tukey's multiple comparison test) was carried out to assess the statistical differences between different groups. GraphPad Prism software (GraphPad Software Inc., La Jolla, CA, USA) was used. Statistical significance was defined at *p*<0.05 for a 95% confidence interval.

Results and discussion

Recently, our group [32] has proposed the combinatorial strategy of tissue engineering principles with nanocarriers towards the intracellular release and regimented supply of Dex aimed at controlling the stem cell osteogenic differentiation in the absence of typical osteogenic cocktails. In the current work, we have investigated the Dex-loaded CMCh/PAMAM dendrimer nanoparticle bone-forming ability, *in vivo*. We therefore exposed RBMSCs to 0.01 mg ml⁻¹ Dex-loaded CMCh/PAMAM dendrimer nanoparticles for 1 week, seeded RBMSCs onto the surface of the HA scaffolds and implanted the constructs subcutaneously on the back of F344/N rats (Fig. 1, top).

The concentration of nanoparticles was chosen considering our previous *in vitro* Dex release profile [32]. These have shown that cultures supplemented with 0.01 mg ml^{-1} Dex-loaded CMCh/PAMAM dendrimer nanoparticles are exposed to $\sim 10 \times 10^{-9} \text{ M}$ Dex, which is in the same magnitude of concentrations to that typically used in osteogenic cocktails for culturing RBMSCs. Moreover, we have shown that these either Dex-loaded or non loaded nanoparticles are internalized by RBMSCs. In another study [35], we demonstrated that osteogenic differentiation occurs in RBMSCs seeded onto the HA scaffolds (3D system) in the presence of 0.01 mg ml^{-1} Dex-loaded CMCh/PAMAM dendrimer nanoparticles, *in vitro*. In this study, the effect of cell number on the bone-forming capacity was also investigated, since it has been shown that it influences ectopic bone formation [37]. Moreover, Ohgushi et al. [46] reported that fresh RBMSCs cultured in the presence of Dex and seeded onto the HA scaffolds can show a high level of *in vivo* bone-forming ability. Thus, RBMSCs/HA constructs, whose freshly isolated RBMSCs were pre-cultured in a MEM medium and MEM medium supplemented with 10^{-8} M Dex were used as controls.

Fig. 1 (bottom) shows a photograph of the RBMSCs/HA construct in the back of the F344/N rats, whose RBMSCs were pre-incubated with 0.01 mg ml^{-1} Dex-loaded CMCh/PAMAM dendrimer nanoparticles, after 4 weeks of subcutaneous implantation. No signs of infection or acute inflammatory reaction were detected at the implantation sites, for all implants. Moreover, we also preliminary assessed by histology, new bone formation on the RBMSCs/HA constructs, after 2 weeks of subcutaneous implantation. At 2 weeks post-implantation no bone formation was detected in the RBMSCs/HA constructs with RBMSCs expanded in the complete MEM medium, MEM medium supplemented with 0.01 mg ml^{-1} Dex-loaded CMCh/PAMAM dendrimer nanoparticles and MEM medium supplemented with 10^{-8} M Dex and HA scaffolds without cells (data not shown).

Fig. 2 shows the 2D μ -CT axial images and respective microradiographs of the RBMSCs/HA constructs after 4 weeks of subcutaneous implantation. The images correspond to the middle section of the HA explants. It is possible to observe different attenuation areas, having high (white), medium (light gray), and low (dark gray) intensities. Thus, we defined the white, light gray, and dark gray areas as HA scaffold, *de novo* bone (NB, gray arrows), and fibrovascular tissue with fat cells, respectively. Massive areas of NB (gray areas) were detected in all RBMSCs/HA scaffold constructs seeded with 1×10^6 RBMSCs (**Figs. 2E, I and M**) as compared to those of HA constructs without cells (**Fig. 2A**) and RBMSCs/HA constructs seeded with 2×10^5 RBMSCs (**Fig. 2C**) pre-cultured in MEM medium.

Fig. 3 reveals the 2D micro-CT axial images of the middle part of HA explants, after applying the threshold 1728–2287, and that is within the range of the predefined threshold set for compact bone in adult (1686–3012). From the figure it is possible to observe the area corresponding to NB (green) formation. We were also able to obtain the 3D architectural data for the NB formed within the explants using the defined threshold (**Table 1**). No bone formation was observed for the HA explants alone (**Fig. 3A**). By its turn, it was observed that few green areas attributed to NB within the RBMSCs/HA constructs seeded with 2×10^5 RBMSCs expanded in MEM medium (**Fig. 3B**). The NB areas in the RBMSCs/HA constructs seeded with 2×10^5 RBMSCs expanded in MEM medium were restricted to the outer surface of the explants, i.e. bone ingrowths in the middle part and core of the HA explants was not observed. Under the micro-CT analysis and using the predefined threshold (within that for compact bone in adult), the volume of NB is about 0. On the contrary, NB formation and ingrowths (osteocondensation) was observed within all sections (top, middle and bottom) of the HA explants seeded with 2×10^5 RBMSCs pre-cultured with Dex and 0.01 mg ml^{-1} Dex-loaded CMCh/PAMAM dendrimer nanoparticles (**Figs. 3D and F**). NB formation and ingrowths (green areas) were also seen in all sections of the RBMSCs/HA scaffold

constructs seeded with 1×10^6 RBMSCs (**Figs. 3C, E, G**). In order to provide further details on NB formation and distribution within the HA explants, a movie for each experimental condition is provided (see **Supplementary data**).

Fig. 4 shows the light microscopy photographs of the different RBMSCs/HA explant decalcified sections after 4 weeks of subcutaneous implantation, which were stained with Haematoxylin and Eosin (H&E). The histological findings showed extensive *de novo* bone formation inside the HA pores with cuboid osteoblasts lining (black arrows) the forming bone matrix in all HA scaffolds seeded with 1×10^6 RBMSCs (**Figs. 4E, F, I, J, M, N**), indicating an active bone formation site. In fact, it is also possible to observe the lacunar spaces and reminiscent osteocyte-like cells entrapped in the bone matrix (see **Figs. 4H, J and L**). Thus, osteocytic lacunae in the lamellar bone are uniform and regularly distributed with osteoblasts forming a continuous layer of bone in a unidirectional way typical of mature bone (NB). In addition, we also detect new bone formation in the HA scaffolds seeded with 2×10^5 RBMSCs that were previously expanded in the presence of 10^{-8} M Dex (**Figs. 4G–H**) and 0.01 mg ml^{-1} Dex-loaded CMCh/PAMAM dendrimer nanoparticles (**Figs. 4K–L**). This data thus confirm that the micro-CT observations in **Figs. 2 and 3** (gray and green areas, respectively) are in fact newly formed bone. From **Figs. 4A–B** it can be seen that fibrovascular tissue (F) with fat cells was formed and that there is no evidence of *de novo* bone formation within the HA scaffolds. No bone formation was observed for the HA explants seeded with 2×10^5 RBMSCs expanded in MEM medium (**Figs. 4C–D**), thus once corroborating the micro-CT findings. Standardized fabrication conditions enabled the production of HA scaffolds with a pore size ranging from 50 to 600 μm , and a mean porosity of $67.8 \pm 5.0\%$. Thus, the present data shows the importance of the porous size and interpore connectivity on the cells in-growth since fibrovascular tissue can be seen in the core of the scaffolds. On the other hand, we can also observe that bone formation within the implants seeded with 1×10^6 RBMSCs pre-cultured in the presence of 10^{-8} M Dex for 7 days, is restricted to the outer part of the HA scaffolds (**Fig. 4I**). In these explants, extensive formation of adipocytes (A) in an inner part of the pores of the implants can be seen. This result is not surprisingly since Porter et al. [27] have shown that the sustained exposure of bone marrow stromal cells to Dex induces the maturation of an adipocyte subpopulation within BMSCs, *in vitro*. In fact, they state that these side effects can be reduced if Dex is supplied in a regimented manner. This hypothesis is supported by our histological findings, since we can detect that the pores of the RBMSCs/HA constructs are completely filled with calcified bone like-matrix (**Fig. 4M**) and the presence of adipocytes is decreased, when RBMSCs are pre-cultured with 0.01 mg ml^{-1} Dex-loaded CMCh/PAMAM dendrimer nanoparticles. Thus, this data supports the idea that the *ex vivo* culturing of RBMSCs with Dex-loaded CMCh/PAMAM dendrimer nanoparticles may be an effective strategy to, on one hand avoid the RBMSCs adipogenic differentiation observed in the inner part of the pores upon withdrawal of dexamethasone and, on the other, direct RBMSCs towards osteogenic differentiation.

Several authors [8,10,48,49] have been considering that degradation rate, pore geometry and degree of interconnectivity are important features to successfully induce *de novo* bone formation, since they control the diffusion of oxygen, nutrients and metabolites to and from the cells. Therefore, the developed HA scaffolds should own an adequate architecture, since extensive new bone formation within the macropores was observed. From 2D micro-CT images and histological observations, new bone connected at the interpore regions (**Figs. 2–4**) can be also observed. This is an important observation as it has been shown that the interpore connections below 3 μm do not allow cell migration and vascularisation [50]. In this study, we were able to observe bone formation in the core of the HA scaffolds, which is an indication that HA scaffolds are osteoconductive and have an adequate interpore size and connection.

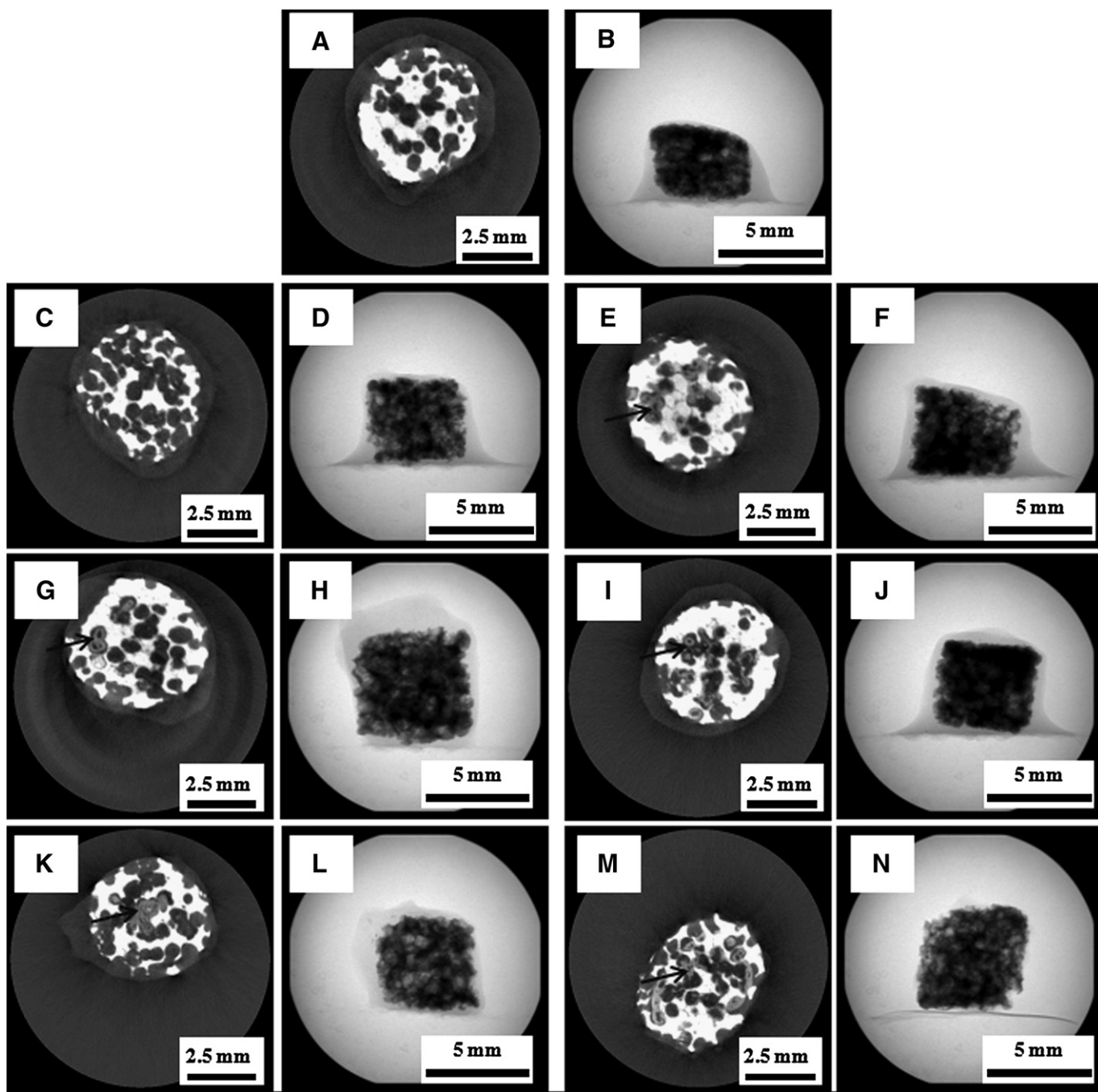


Fig. 2. 2D micro-CT axial images of the explants (middle sections) and respective X-ray photographs, after 4 weeks of subcutaneous implantation: HA scaffolds (A–B), HA seeded with 2×10^5 RBMSCs which were expanded in MEM medium (C–D), HA seeded with 1×10^6 RBMSCs which were expanded in MEM medium (E–F), HA seeded with 2×10^5 RBMSCs which were expanded in MEM medium supplemented with 10^{-8} M dexamethasone (G–H), HA seeded with 1×10^6 RBMSCs which were expanded in MEM medium supplemented with 10^{-8} M dexamethasone (I–J), HA seeded with 2×10^5 RBMSCs which were expanded in MEM medium supplemented with 0.01 mg ml^{-1} Dex-loaded CMCh/PAMAM dendrimer nanoparticles (K–L), and HA seeded with 1×10^6 RBMSCs which were expanded in MEM medium supplemented with 0.01 mg ml^{-1} Dex-loaded CMCh/PAMAM dendrimer nanoparticles (M–N). We defined the white, light gray, and dark gray areas as HA scaffold, new bone formation (black arrows), and fibrovascular tissue with fat cells, respectively.

Fig. 5A shows a representative light microscopy photograph of a decalcified section (H&E staining) of HA scaffolds seeded with 1×10^6 RBMSCs which were expanded in MEM medium supplemented with 0.01 mg ml^{-1} Dex-loaded CMCh/PAMAM dendrimer nanoparticles, after 4 weeks of subcutaneous implantation. **Figs. 5B–D** show the respective imaging processing that was carried out to perform the histomorphometrical analyses. The 2D histological section images were converted to gray-value images and several filter steps were performed [47]. Shrinkage percentage observed in decalcified sections was not considered in the calculations of the percentage of bone

volume density (BV/TSV). Therefore some care should be taken when comparing this data with the 3D architectural data obtained using micro-CT.

Table 1 shows the percentage of BV/TSV in the different implants determined from the histomorphometrical analyses of the 2D histological sections and 3D bone volume obtained using the micro-CT. The histomorphometrical results using a threshold have shown that no bone formation was observed in the HA scaffolds without RBMSCs and HA seeded with 2×10^5 RBMSCs expanded in MEM medium. Bone volume density in HA seeded with 1×10^6 RBMSCs expanded in MEM medium

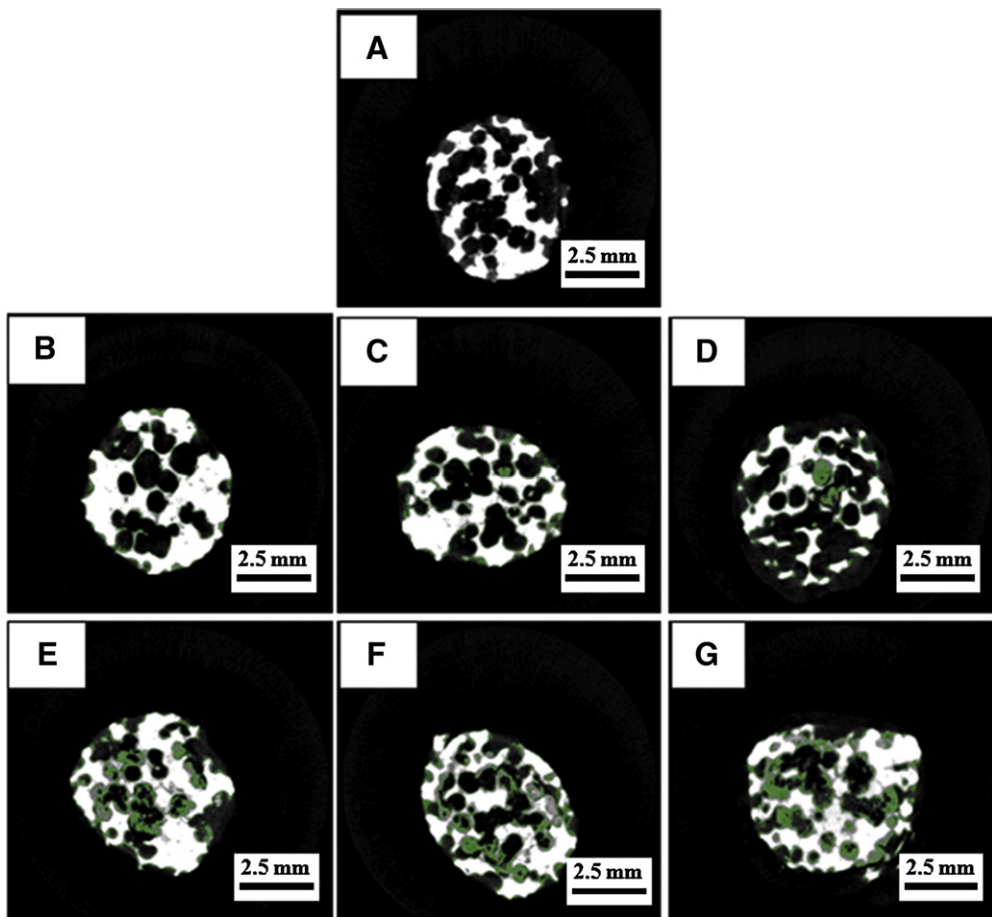


Fig. 3. 2D micro-CT axial images of the explants (middle sections) to which was applied a threshold of 1728–2287, after 4 weeks of subcutaneous implantation: HA scaffolds (A), HA seeded with 2×10^5 RBMSCs which were expanded in MEM medium (B), HA seeded with 1×10^6 RBMSCs which were expanded in MEM medium (C), HA seeded with 2×10^5 RBMSCs which were expanded in MEM medium supplemented with 10^{-8} M dexamethasone (D), HA seeded with 1×10^6 RBMSCs which were expanded in MEM medium supplemented with 10^{-8} M dexamethasone (E), HA seeded with 2×10^5 RBMSCs which were expanded in MEM medium supplemented with 0.01 mg ml^{-1} Dex-loaded CMCh/PAMAM dendrimer nanoparticles (F), and HA seeded with 1×10^6 RBMSCs which were expanded in MEM medium supplemented with 0.01 mg ml^{-1} Dex-loaded CMCh/PAMAM dendrimer nanoparticles (G).

was $27.1 \pm 7.1\%$. By its turn, HA seeded with 2×10^5 and 1×10^6 RBMSCs expanded in MEM medium supplemented with 10^{-8} M Dex was $6.9 \pm 4.7\%$ and $36.4 \pm 9.2\%$, respectively. Finally, HA seeded with 2×10^5 and

1×10^6 RBMSCs expanded in MEM medium supplemented with 0.01 mg ml^{-1} Dex-loaded CMCh/PAMAM dendrimer nanoparticles was $30.5 \pm 6.0\%$ and $38.1 \pm 5.7\%$, respectively. These results have

Table 1
Percentage of bone volume density (BV/TSV) calculated from the histomorphometrical analyses of the 2D histological sections of the different explants, after 4 weeks of subcutaneous implantation. A minimum of 12 sections per explant were analyzed. The bone volume (3D analysis) formed within the explants was also quantified using micro-CT technique using a contrast between 1001 and 4080 and a threshold of 1728–2287. The threshold used to quantify the new bone formed was within the range of the micro-CT thresholding for compact bone in adult (1686–3012). A movie for each explant is provided as *Supplementary data*.

Explant	Histological sections % Bone volume density (mean \pm std. dev.)	Micro-CT % Bone volume density (mean \pm std. dev.)
HA scaffolds without RBMSCs	0	0
HA seeded with 2×10^3 RBMSCs expanded in MEM medium	0	0
HA seeded with 2×10^5 RBMSCs expanded in MEM medium supplemented with 10^{-8} M Dex	6.9 ± 4.7	0.31 ± 0.14
HA seeded with 2×10^5 RBMSCs expanded in MEM medium supplemented with 0.01 mg ml^{-1} Dex-loaded CMCh/PAMAM dendrimer nanoparticles	30.5 ± 6.0	0.72 ± 0.01
HA seeded with 2×10^6 RBMSCs expanded in MEM medium	27.1 ± 7.1	0.52 ± 0.38
HA seeded with 1×10^6 RBMSCs expanded in MEM medium supplemented with 10^{-8} M Dex	36.4 ± 9.2	0.58 ± 0.38
HA seeded with 1×10^6 RBMSCs expanded in MEM medium supplemented with 0.01 mg ml^{-1} Dex-loaded CMCh/PAMAM dendrimer nanoparticles	38.1 ± 5.7	0.95 ± 0.09

p value: *** <0.001 ; ** <0.01 ; and * <0.05 .

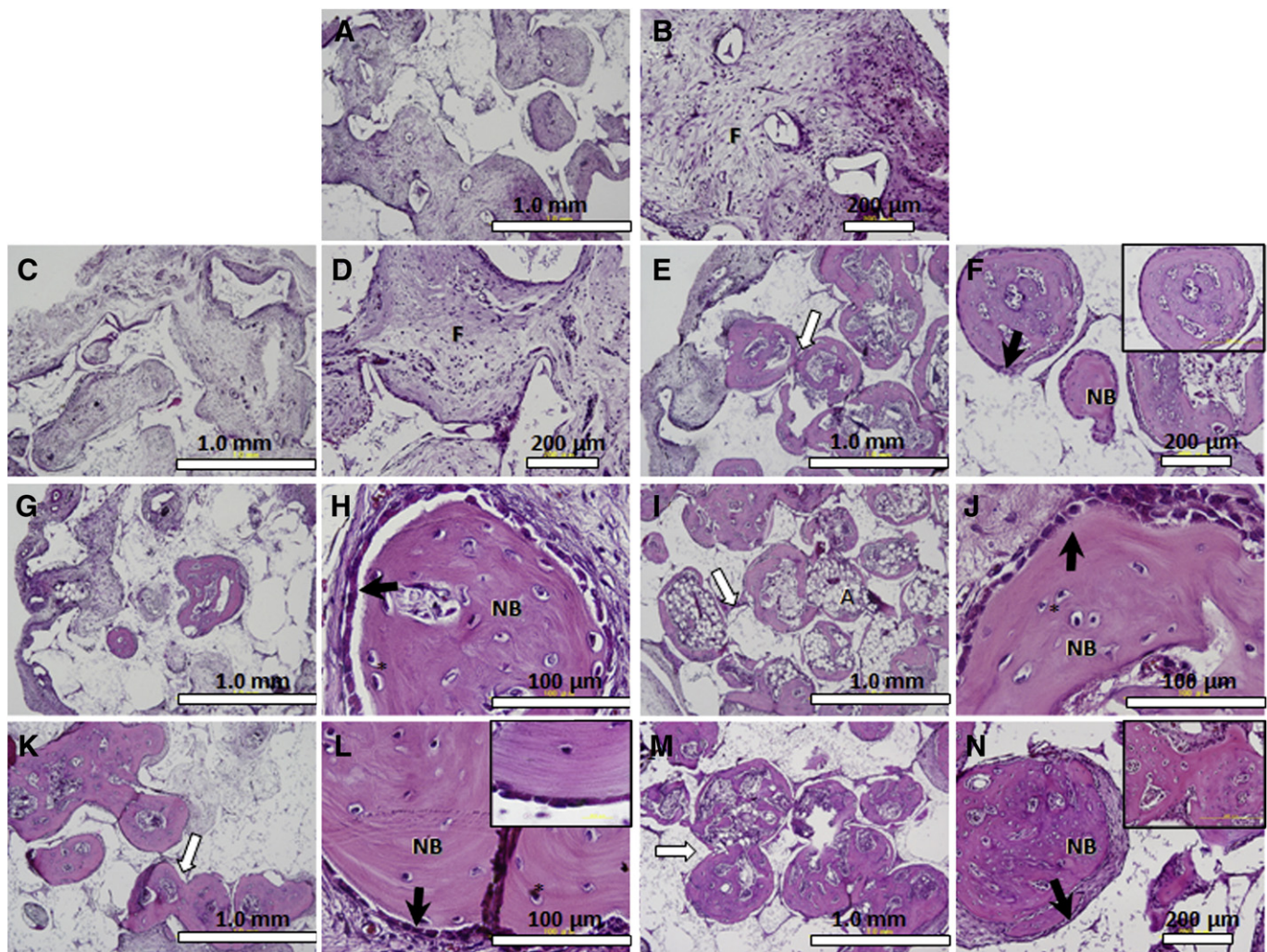


Fig. 4. Light microscopy photographs of the explants sections stained with Haematoxylin and Eosin (decalcified sections), after 4 weeks of subcutaneous implantation: HA scaffolds (A–B), HA seeded with 2×10^5 RBMSCs which were expanded in MEM medium (C–D), HA seeded with 1×10^6 RBMSCs which were expanded in MEM medium (E–F), HA seeded with 2×10^5 RBMSCs which were expanded in MEM medium supplemented with 10^{-8} M dexamethasone (G–H), HA seeded with 1×10^6 RBMSCs which were expanded in MEM medium supplemented with 10^{-8} M dexamethasone (I–J), HA seeded with 2×10^5 RBMSCs which were expanded in MEM medium supplemented with 0.01 mg ml^{-1} Dex-loaded CMCh/PAMAM dendrimer nanoparticles (K–L), and HA seeded with 1×10^6 RBMSCs which were expanded in MEM medium supplemented with 0.01 mg ml^{-1} Dex-loaded CMCh/PAMAM dendrimer nanoparticles (M–N). It is possible to observe representative areas of *de novo* bone formation (NB), fibrous tissue (F) and adipocytes (A). White arrows indicate the interconnected pores. Black arrows show the cell lining which is suggestive of active osteoblasts. Osteocytes can also be visualized (*).

demonstrated that there is a significant increase ($p < 0.01$) in NB within HA seeded with 1×10^6 RBMSCs pre-cultured with 0.01 mg ml^{-1} Dex-loaded CMCh/PAMAM dendrimer nanoparticles as compared to HA seeded with 2×10^5 RBMSCs pre-cultured with 0.01 mg ml^{-1} Dex-loaded CMCh/PAMAM dendrimer nanoparticles. A significant increase ($p < 0.001$) in NB within HA seeded with 2×10^5 RBMSCs pre-cultured with 0.01 mg ml^{-1} Dex-loaded CMCh/PAMAM dendrimer nanoparticles can also be seen as compared to both HA explants seeded with 2×10^5 RBMSCs pre-cultured with Dex and seeded with 2×10^5 RBMSCs pre-cultured in MEM. These results revealed that cell number and culture conditions are critical factors in promoting *de novo* bone formation, *in vivo*. These results are corroborated by the non-destructive micro-CT analyses (bone volume), which have shown that no bone formation was observed in the HA explants without RBMSCs and HA explants seeded with 2×10^5 RBMSCs pre-cultured in MEM medium.

The present data revealed that porous HA ceramics alone do not induce bone formation upon subcutaneous implantation in the back of the F344/N rats. However, bone formation could be detected by seeding RBMSCs onto the HA scaffolds, when the cell number used was 1×10^6 cells. Moreover, our findings corroborates previous ones

[22–24], as it demonstrated once the need of cells to be exposed to Dex for promoting *de novo* bone formation. Despite, in this work we have shown that Dex-loaded CMCh/PAMAM dendrimer nanoparticles induced a superior new bone formation as compared to that of RBMSCs expanded in MEM medium supplemented with 10^{-8} M Dex, the typical concentration used in osteogenic media [44]. This was particularly evident and statistically significant when seeding 2×10^5 RBMSCs onto the surface of the HA scaffolds. Our present data is relevant if we consider that, to our knowledge, no reports have shown pores of implanted ceramics completely filled with newly formed bone when seeded with low cell numbers, after 4 weeks of implantation. For example, Nishikawa et al. [10] observed that bone formation in the RBMSCs/HA scaffolds after 2 weeks of ectopic implantation occurred, but constructs were previously cultured *in vitro* in an osteogenic medium. By its turn, Arinze et al. [8] observed low amounts of new bone formation in the HA scaffolds seeded with 5×10^6 cells, and mainly restricted to peripheral pores, after 6 weeks.

It has been reported [27,51,52] that sustained exposure of bone marrow stromal cells to Dex down-regulate collagen type I production *in vitro*, both in humans and animal models. To further investigate

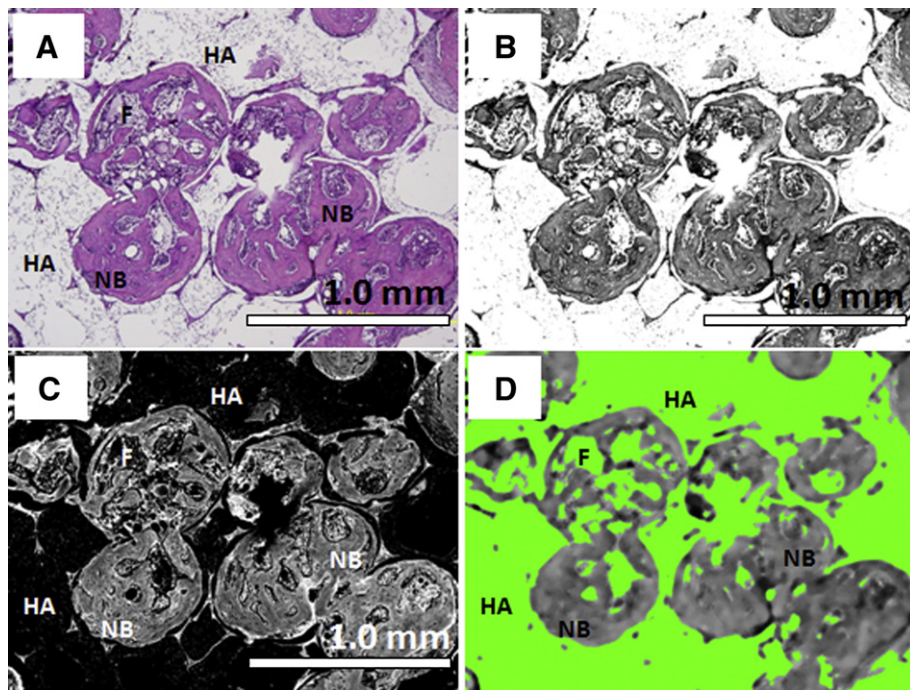


Fig. 5. Light microscopy photographs of an explant section corresponding to the HA seeded with 1×10^6 RBMSCs which were expanded in MEM medium supplemented with 0.01 mg ml^{-1} Dex-loaded CMCh/PAMAM dendrimer nanoparticles, after 4 weeks of subcutaneous implantation: decalcified section stained with Haematoxylin and Eosin (A), and respective imaging processing (B–D). It is possible to observe representative areas of *de novo* bone formation (NB), HA scaffolds (HA) and fibrous tissue (F).

proteoglycan extracellular matrix synthesis (ECM) [37], we stained the explant sections with the methacromatic Toluidine blue (Fig. 6). Methacromasia was weakly observed in implants where new bone formation was formed (Figs. 6E–F, G–H, I–J, and K–L). The other explants had no such findings (Figs. 6A–B, and C–D). However, enhanced methacromasia was evident within HA explants seeded with RBMSCs pre-cultured in the presence of 0.01 mg ml^{-1} Dex-loaded CMCh/PAMAM dendrimer nanoparticles (Figs. 6M–N), which shows the ECM rich of proteoglycans. This data suggests that supplying Dex in a regimented manner can enhance proteoglycan extracellular matrix synthesis. No cartilaginous like-matrix [53] was observed.

Osteoblast differentiation is accompanied by the differential and temporal expression of several osteoblastic markers such as ALP, osteopontin, collagen type I, and osteocalcin [39]. In order to demonstrate the osteogenic capacity of the different explants quantitatively, we measured the ALP activity and osteocalcin contents, after 4 weeks of implantation. Fig. 7 shows the ALP activity and osteocalcin content of the HA scaffolds without RBMSCs and the several RBMSCs/HA construct explants. As seen for bone formation, the ALP activity is significantly higher ($p < 0.001$) in all the HA explants seeded with 1×10^6 RBMSCs as compared to that seeded with 2×10^5 RBMSCs (Fig. 7a). This data thus suggests that osteogenic differentiation did occur in cultures with and without Dex, which corroborates previous histological findings. It can be seen that ALP is significantly higher ($p < 0.001$) when RBMSCs were expanded in a culture medium with 0.01 mg ml^{-1} Dex-loaded CMCh/PAMAM dendrimer nanoparticles and 10^{-8} M Dex as compared to explants whose RBMSCs were expanded in MEM medium. In addition, no significant differences were observed among the explants seeded with 1×10^6 RBMSCs whose cells were expanded in a culture medium with Dex-loaded CMCh/PAMAM dendrimer nanoparticles and 10^{-8} M Dex. Significant differences in ALP activity were observed among the explants seeded with 2×10^5 RBMSCs. It can be seen that ALP activity in the explants where RBMSCs were expanded in a culture medium with 0.01 mg ml^{-1} Dex-loaded CMCh/PAMAM dendrimer nanoparticles presented significantly higher ($p < 0.05$) ALP levels as compared to that of culture medium

whose RBMSCs were both pre-cultured with 10^{-8} M Dex and MEM, which is consistent with the higher bone formation observed. In other words, our data are in full agreement with previous findings [26,54], as we found that a continuous treatment with Dex consistently increases the ALP activity, which is an indication of the osteogenic commitment of RBMSCs. Thus, it can be seen that Dex induced the early osteoblastic differentiation and potentiate new bone formation. Moreover, HA scaffolds without RBMSCs and RBMSC/HA constructs seeded with 2×10^5 RBMSCs expanded in MEM medium showed decreased ALP activity, which once corroborates our findings on the important role of both Dex supply and cell number in promoting *de novo* bone formation.

Fig. 7b shows osteocalcin content of the RBMSCs/HA constructs explants, after 4 weeks of subcutaneous implantation. Osteocalcin content is significantly higher when RBMSCs were expanded in culture medium with 0.01 mg ml^{-1} Dex-loaded CMCh/PAMAM dendrimer nanoparticles as compared to HA explants where RBMSCs were cultured in MEM medium. The increase in osteocalcin expression indicates an advancing differentiation. Similarly to what was observed for ALP activity, osteocalcin content in the HA explants without cells is significantly decreased as compared to all HA explants with seeded RBMSCs. In addition, it is possible to observe that osteocalcin content did not vary significantly in the explants seeded with different cell numbers but pre-cultured in identical culture conditions (B–C). Moreover, no significant difference in osteocalcin content was found in HA explants with RBMSCs exposed to Dex as compared to HA explants seeded with RBMSCs pre-cultured with 0.01 mg ml^{-1} Dex-loaded CMCh/PAMAM dendrimer nanoparticles. These results can be explained by the unresponsiveness of osteocalcin to long-term exposure to Dex in our experimental study as this late osteoblastic marker appears to reach a maximum just before or during mineralized tissue formation [55]. In addition, it has been shown [56,57] that the expression of osteocalcin increases with mineral deposition, while ALP levels decreases. Another possible explanation for our findings has been advanced by Porter et al. [27], which demonstrated that Dex induces the expression of bone sialoprotein, but not osteocalcin. Thus, osteocalcin expression may be stimulated

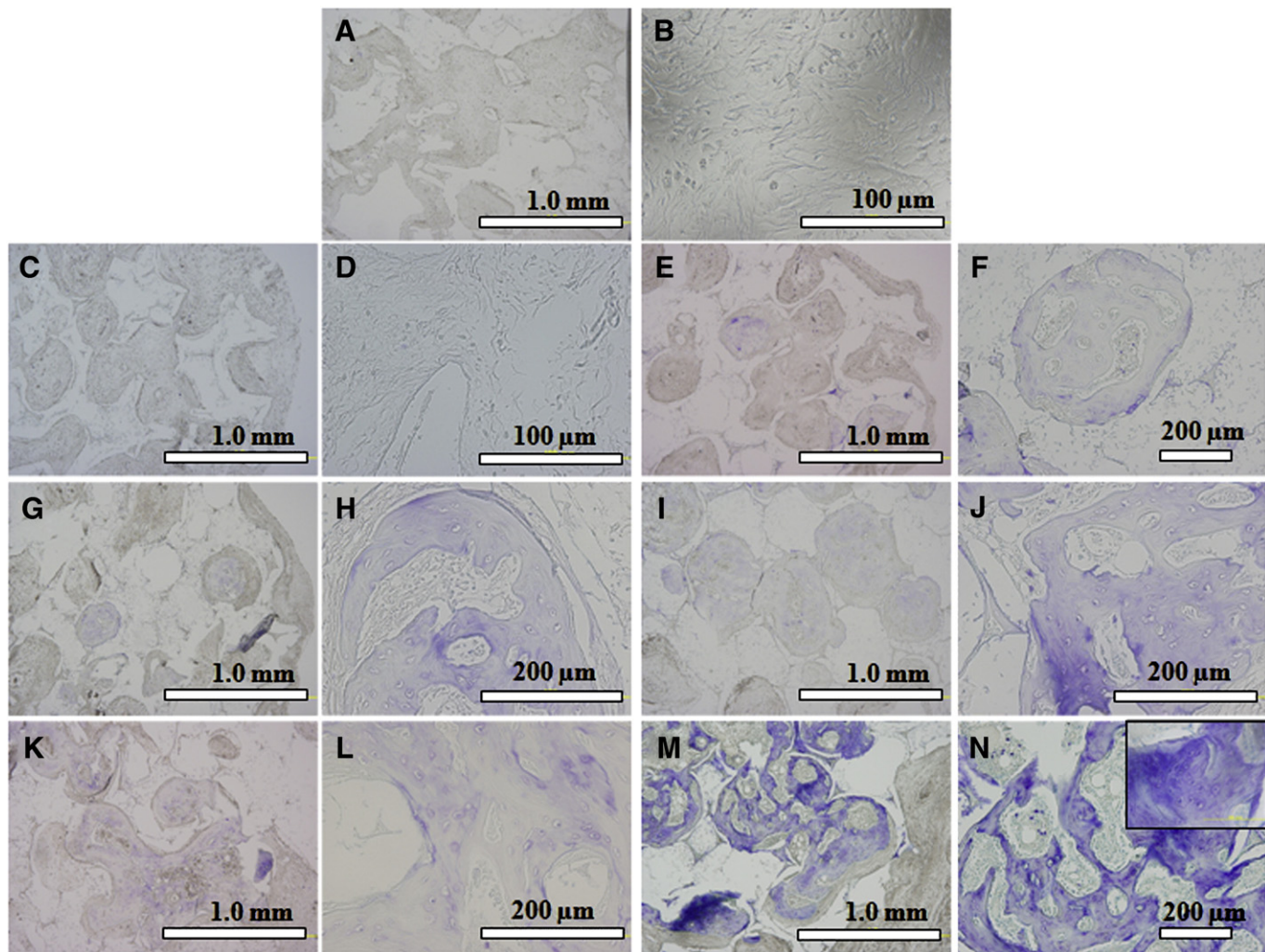


Fig. 6. Light microscopy photographs of the different explants sections stained with Toluidine blue staining (decalcified sections), after 4 weeks of subcutaneous implantation: HA scaffolds (A–B), HA seeded with 2×10^5 RBMSCs which were expanded in MEM medium (C–D), HA seeded with 1×10^6 RBMSCs which were expanded in MEM medium (E–F), HA seeded with 2×10^5 RBMSCs which were expanded in MEM medium supplemented with 10^{-8} M dexamethasone (G–H), HA seeded with 1×10^6 RBMSCs which were expanded in MEM medium supplemented with 10^{-8} M dexamethasone (I–J), HA seeded with 2×10^5 RBMSCs which were expanded in MEM medium supplemented with 0.01 mg ml^{-1} Dex-loaded CMCh/PAMAM dendrimer nanoparticles (K–L), and HA seeded with 1×10^6 RBMSCs which were expanded in MEM medium supplemented with 0.01 mg ml^{-1} Dex-loaded CMCh/PAMAM dendrimer nanoparticles (M–N). It is possible to observe representative weak and strong methacrosia for proteoglycan extracellular matrix (ECM), in explants where new bone formation was detected.

through a different pathway. Despite, these results confirmed the osteogenic capacity of the HA scaffolds seeded with 1×10^6 RBMSCs and supported the fact that exposure of Dex prior and during implantation time can result in a superior *de novo* bone formation. Moreover, this study supported previous ones [32,35], and showed that CMCh/PAMAM dendrimer nanoparticles can supply Dex to RBMSCs, thus acting at both early and late stages to direct proliferative osteoprogenitor cells toward terminal maturation. The superior role of Dex-loaded CMCh/PAMAM dendrimer nanoparticles towards enhancing ALP levels was particularly evident when seeding 2×10^5 RBMSCs per HA scaffold. Despite the interesting data, we envision performing *in vivo* studies for longer implantation periods to clarify further, the effect of the regimented supply of Dex delivered via Dex-loaded CMCh/PAMAM dendrimer nanoparticles versus withdrawal of Dex on the osteogenic differentiation and bone-forming ability of the RBMSCs.

In conclusion, this work demonstrated that cell number and *ex vivo* culturing strategies greatly influence the osteogenesis and *de novo* bone formation, *in vivo*. RBMSCs expanded with 0.01 mg ml^{-1} dexamethasone-loaded carboxymethylchitosan/poly(amidoamine) dendrimer nanoparticles and seeded at low cell number on the

surface of the HA scaffolds enhanced the ectopic bone formation, after 4 weeks of subcutaneous implantation in the back of Fischer 344 rats. This study reveals that the novel dexamethasone-loaded carboxymethylchitosan/poly(amidoamine) dendrimer nanoparticles may be beneficial as intracellular nanocarrier and supply of Dex aimed at modulate and direct stem cell differentiation towards osteogenic phenotype, enhance proteoglycan extracellular matrix synthesis and superior ectopic *de novo* bone formation. Moreover, the architecture of HA scaffolds proved to be an adequate support for osteogenic differentiation of bone marrow derived osteoblast and bone formation, *in vivo*. Thus, in this work it has been demonstrated that the innovative tissue engineering strategy proposed is effective on promoting *de novo* bone formation *in vivo* and avoid the need of culturing stromal cells in the presence of typical osteogenic cocktails, prior to implantation.

Acknowledgments

This study was supported by the Portuguese Foundation for Science and Technology (FCT) through POCTI and FEDER programmes (SFRH/BD/21786/2005) and by the Canon Foundation in Europe. We

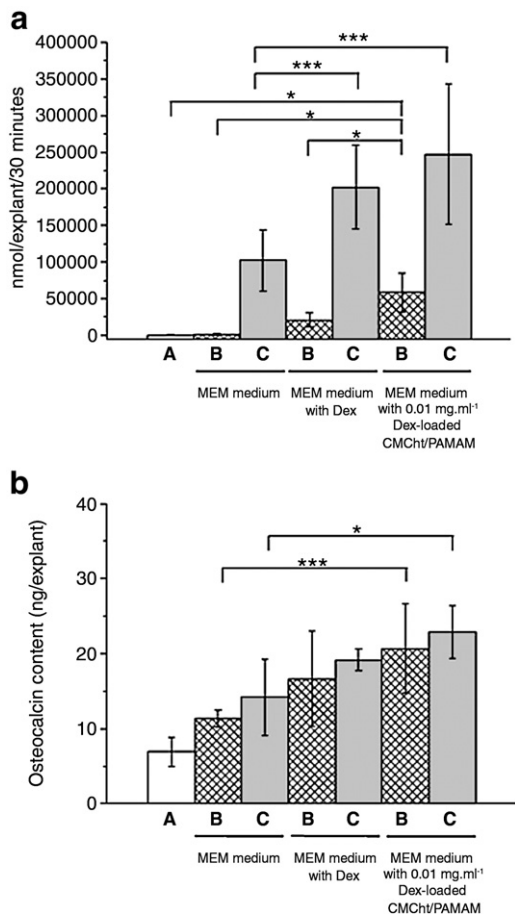


Fig. 7. ALP activity (a) and osteocalcin content (b) of the different explants after 4 weeks of subcutaneous implantation: HA scaffolds (A), HA seeded with 2×10^5 RBMSCs (B), HA seeded with 1×10^6 RBMSCs (C). Results expressed as an average \pm standard deviation, $n=9$ (p value: *** <0.001 , ** <0.01 ; * <0.05).

wish to thank P.B. Malafaya for the technical support during the micro-CT analyses, and to Materialise for providing the Mimics® software. This work was also supported by the European Union funded STREP Project HIPPOCRATES (NMP3-CT-2003-505758) and European NoE EXPERTISSUES (NMP3-CT-2004-500283).

Appendix A. Supplementary data

Supplementary data associated with this article can be found, in the online version, at doi: [10.1016/j.bone.2010.02.007](https://doi.org/10.1016/j.bone.2010.02.007).

References

- Chu TMG, Orton DG, Hollister SJ, Feinberg SE, Halloran JW. Mechanical and *in vivo* performance of hydroxyapatite implants with controlled architectures. *Biomaterials* 2002;23(5):1283–93.
- Schnettler R, Alt V, Dingeldein E, Pfefferle H-J, Kilian O, Meyer C, et al. Bone ingrowth in bFGF-coated hydroxyapatite ceramic implants. *Biomaterials* 2003;24(25):4603–8.
- Jones AC, Arns CH, Sheppard AP, Hutmacher DW, Milthorpe BK, Knackstedt MA. Assessment of bone ingrowth into porous biomaterials using micro-CT. *Biomaterials* 2007;28(15):2491–504.
- Woodard JR, Hilldore AJ, Lan SK, Park CJ, Morgan AW, Eurell JAC, et al. The mechanical properties and osteoconductivity of hydroxyapatite bone scaffolds with multi-scale porosity. *Biomaterials* 2007;28(1):45–54.
- Boyde A, Corsi A, Quarto R, Cancedda R, Bianco P. Osteoconduction in large macroporous hydroxyapatite ceramic implants: evidence for a complementary integration and disintegration mechanism. *Bone* 1999;24(6):579–89.
- Kozo O, Yamamoto T, Nakamura T, Kokubo T. Quantitative study on osteoconduction of apatite-wollastonite containing glass ceramic granules, hydroxyapatite granules and alumina granules. *Biomaterials* 1990;11(4):265–71.
- Kurashina K, Kurita H, Takeuchi H, Hirano N, Klein CPAT, de Groot K. Osteogenesis in muscle with composite graft of hydroxyapatite and autogenous calvarial periosteum: a preliminary report. *Biomaterials* 1995;16(2):119–23.
- Arinzech TL, Tran T, McAlary J, Daculsi G. A comparative study of biphasic calcium phosphate ceramics for human mesenchymal stem-cell-induced bone formation. *Biomaterials* 2005;26(17):3631–8.
- Kim H, Suh H, Jo SA, Kim HW, Lee JM, Kim EH, et al. *In vivo* bone formation by human marrow stromal cells in biodegradable scaffolds that release dexamethasone and ascorbate-2-phosphate. *Biochem Biophys Res Commun* 2005;332(4):1053–60.
- Nishikawa M, Myoui A, Ohgushi H, Ikeuchi M, Tamai N, Yoshikawa H. Bone Tissue engineering using novel interconnected porous hydroxyapatite ceramics combined with marrow mesenchymal cells: quantitative and three-dimensional image analysis. *Cell Transplant* 2004;13:367–76.
- Uemura T, Dong J, Wang Y, Kojima H, Saito T, Iejima D, et al. Transplantation of cultured bone cells using combinations of scaffolds and culture techniques. *Biomaterials* 2003;24(13):2277–86.
- Hosseinkhani H, Yamamoto M, Inatsugu Y, Hiraoka Y, Inoue S, Shimokawa H, et al. Enhanced ectopic bone formation using a combination of plasmid DNA impregnation into 3-D scaffold and bioreactor perfusion culture. *Biomaterials* 2006;27(8):1387–98.
- Kruyt MC, Dhert WJA, Oner FC, van Blitterswijk CA, Verbout AJ, de Brujin JD. Analysis of ectopic and orthotopic bone formation in cell-based tissue-engineered constructs in goats. *Biomaterials* 2007;28(10):1798–805.
- Srouji S, Livne E. Bone marrow stem cells and biological scaffold for bone repair in aging and disease. *Mech Ageing Dev* 2005;126(2):281–7.
- Bianco P, Robey PG. Stem cells in tissue engineering. *Nature* 2001;414:118–21.
- Karussis D, Kassis I, Kurkali BGS, Slavin S. Immunomodulation and neuroprotection with mesenchymal bone marrow stem cells (MSCs): a proposed treatment for multiple sclerosis and other neuroimmunological/neurodegenerative diseases. *J Neurol Sci* 2008;265(1–2):131–5.
- Hou M, Yang K-M, Zhang H, Zhu W-Q, Duan F-J, Wang H, et al. Transplantation of mesenchymal stem cells from human bone marrow improves damaged heart function in rats. *Int J Cardiol* 2007;115(2):220–8.
- Liu W, Cui L, Cao Y, Klimanskaya Irina, Robert L. Bone reconstruction with bone marrow stromal cells. *Methods in enzymology*. Academic Press; 2006. p. 362.
- Banfi A, Muraglia A, Dozin B, Mastrogiammo M, Cancedda R, Quarto R. Proliferation kinetics and differentiation potential of *ex vivo* expanded human bone marrow stromal cells: implications for their use in cell therapy. *Exp Hematol* 2000;28(6):707–15.
- Krampera M, Pizzolo G, Aprili G, Franchini M. Mesenchymal stem cells for bone, cartilage, tendon and skeletal muscle repair. *Bone* 2006;39(4):678–83.
- Mauney JR, Jaquiere C, Volloch V, Heberer M, Martin I, Kaplan DL. *In vitro* and *in vivo* evaluation of differentially demineralized cancellous bone scaffolds combined with human bone marrow stromal cells for tissue engineering. *Biomaterials* 2005;26(16):3173–85.
- Ogston N, Harrison AJ, Cheung HFJ, Ashton BA, Hampson G. Dexamethasone and retinoic acid differentially regulate growth and differentiation in an immortalised human clonal bone marrow stromal cell line with osteoblastic characteristics. *Steroids* 2002;67:895–906.
- Eijken M, Koedam M, van Driel M, Buurman CJ, Pols HAP, van Leeuwen JPTM. The essential role of glucocorticoids for proper human osteoblast differentiation and matrix mineralization. *Mol Cell Endocrinol* 2006;248:87–93.
- Blum JS, Brandon Parrott M, Mikos AG, Barry MA. Early osteoblastic differentiation induced by dexamethasone enhances adenoviral gene delivery to marrow stromal cells. *J Orthop Res* 2004;22(2):411–6.
- Jorgensen NR, Henriksen Z, Sorensen OH, Civitelli R. Dexamethasone, BMP-2, and 1, 25-dihydroxyvitamin D enhance a more differentiated osteoblast phenotype: validation of an *in vitro* model for human bone marrow-derived primary osteoblasts. *Steroids* 2004;69(4):219–26.
- Holtorf HL, Jansen JA, Mikos AG. Ectopic bone formation in rat marrow stromal cell/titanium fiber mesh scaffold constructs: effect of initial cell phenotype. *Biomaterials* 2005;26(31):6208–16.
- Porter RM, Huckle WR, Goldstein AS. Effect of dexamethasone withdrawal on osteoblastic differentiation of bone marrow stromal cells. *J Cell Biochem* 2003;90:13–22.
- Castano-Izquierdo H, Alvarez-Barreto J, van den Dolder J, Jansen JA, Mikos AG, Sikavitsas VI. Pre-culture period of mesenchymal stem cells in osteogenic media influences their *in vivo* bone forming potential. *J Biomed Mater Res, Part A* 2007;82:129–38.
- Mountzaris PM, Mikos AG. Modulation of the inflammatory response for enhanced bone tissue regeneration. *Tissue Eng, Part B* 2008;14:179–86.
- Hayashi R, Wada H, Ito K, Adcock IM. Effects of glucocorticoids on gene transcription. *Eur J Pharmacol* 2004;500:51–62.
- Schäck H, Döcke WD, Asadullah K. Mechanisms involved in the side effects of glucocorticoids. *Pharmacol Ther* 2002;96:23–43.
- Oliveira JM, Kotobuki N, Marques AP, Pirraco RP, Benesch J, Hirose M, et al. Surface engineered carboxymethylchitosan/poly(amidoamine) dendrimer nanoparticles for intracellular targeting. *Adv Funct Mater* 2008;18:1840–53.
- Oliveira JM, Kotobuki N, Hirose M, Mano JF, Reis RL, Ohgushi H, editors. *Intracellular Carboxymethylchitosan/Poly(amidoamine) Nanocarriers Loaded with Dexamethasone Enhances Osteogenic Differentiation of RBMSCs In Vitro*. Tissue Eng; 2007. p. 1719. London, UK.
- Oliveira JM, Silva SS, Malafaya PB, Rodrigues MT, Gomes ME, Kotobuki N, et al. Macroporous hydroxyapatite scaffolds for bone tissue engineering applications: physicochemical characterization and assessment of rat bone marrow stromal cells viability. *J Biomed Mater Res, Part A* 2009;91(1):175–86.

- [35] Oliveira JM, Sousa RA, Kotobuki N, Tadokoro M, Hirose M, et al. The osteogenic differentiation of rat bone marrow stromal cells cultured with dexamethasone-loaded carboxymethylchitosan/poly(amidoamine) dendrimer nanoparticles. *Biomaterials* 2008;30(5):804–13.
- [36] Ito A, Ohtsuka M, Kawamura H, Ikeuchi M, Ohgushi H, Sogo Y, et al. Zinc-containing tricalcium phosphate and related materials for promoting bone formation. *Curr Appl Phys* 2005;5:402–6.
- [37] Kasten P, Vogel J, Luginbuhl R, Niemeyer P, Tonak M, Lorenz H, et al. Ectopic bone formation associated with mesenchymal stem cells in a resorbable calcium deficient hydroxyapatite carrier. *Biomaterials* 2005;26(29):5879–89.
- [38] Haynesworth SE, Goshima J, Goldberg VM, Caplan AI. Characterization of cells with osteogenic potential from human marrow. *Bone* 1992;13:81–8.
- [39] Beck GR, Zerler B, Moran E. Phosphate is a specific signal for induction of osteopontin gene expression. *Proc Natl Acad Sci* 2000;97:8352–7.
- [40] Harris H. The human alkaline phosphatases: what we know and what we don't know. *Clin Chim Acta* 1989;186:133–50.
- [41] Oliveira JM, Silva SS, Mano JF, Reis RL. Innovative technique for the preparation of porous bilayer hydroxyapatite/chitosan scaffolds for osteochondral applications. Kyoto (JPN): Key Eng Mater, Trans Tech Pub; 2006. p. 927–30. Zurich, Switzerland.
- [42] Oliveira JM, Rodrigues MT, Silva SS, Malafaya PB, Gomes ME, Viegas CA, et al. Novel hydroxyapatite/chitosan bilayered scaffold for osteochondral tissue-engineering applications: scaffold design and its performance when seeded with goat bone marrow stromal cells. *Biomaterials* 2006;27(36):6123–37.
- [43] Chen X-G, Park H-J. Chemical characteristics of O-carboxymethyl chitosans related to the preparation conditions. *Carbohydr Polymer* 2003;53:355–9.
- [44] Kihara T, Oshima A, Hirose M, Ohgushi H. Three-dimensional visualization analysis of *in vitro* cultured bone fabricated by rat marrow mesenchymal stem cells. *Biochem Biophys Res Commun* 2004;316:943–8.
- [45] Kotobuki N, Motohiro H, Machida H, Katou Y, Muraki K, Takakura Y, et al. Viability and osteogenic potential of cryopreserved human bone marrow-derived mesenchymal cells. *Tissue Eng* 2005;11:663–73.
- [46] Tadokoro M, Hattori Y, Ohgushi H. Rapid preparation of fresh frozen tissue-engineered bone sections for histological, histomorphometrical and histochemical analyses. *Biomed Mater Eng* 2006;16:405–13.
- [47] Muller R, Van Campenhout H, Van Damme B, Van der Perre G, Dequeker J, Hildebrand T, et al. Morphometric analysis of human bone biopsies: a quantitative structural comparison of histological sections and micro-computed tomography. *Bone* 1998;23(1):59–66.
- [48] Zeltinger J, Sherwood JK, Graham DA, Mueller R, Griffith LG. Effect of pore size and void fraction on cellular adhesion, proliferation, and matrix deposition. *Tissue Eng* 2001;7:557–72.
- [49] Simon JL, Roy TD, Parsons JR, Rekow ED, Thompson VP, Kemnitzer J, et al. Engineered cellular response to scaffold architecture in a rabbit trephine defect. *J Biomed Mater Res, Part A* 2003;66A:275–82.
- [50] Tamai N, Myoui A, Tomita T, Nakase T, Tanaka J, Ochi T, et al. Novel hydroxyapatite ceramics with an interconnective porous structure exhibit superior osteoconduction *in vivo*. *J Biomed Mater Res* 2002;59:110–7.
- [51] Hicok KC, Thomas T, Gori F, Rickard DJ, Spelsberg TC, Riggs BL. Development and characterisation of conditionally immortalised osteoblast precursor cell lines from human bone marrow stroma. *J Bone Miner Res* 1998;13:205–17.
- [52] Mahonen A, Jukkola A, Risteli L, Risteli J, Maenpaa PH. Type 1 procollagen synthesis is regulated by steroids and related hormones in human osteosarcoma cells. *J Cell Biochem* 1998;68:151–63.
- [53] Chen G, Liu D, Tadokoro M, Hirochika R, Ohgushi H, Tanaka J, et al. Chondrogenic differentiation of human mesenchymal stem cells cultured in a cobweb-like biodegradable scaffold. *Biochem Biophys Res Commun* 2004;322(1):50–5.
- [54] Wong MM, Rao LG, Ly H, Hamilton L, Tong J, Sturridge W, et al. Long-term effects of physiologic concentrations of dexamethasone on human bone-derived cells. *J Bone Miner Res* 1990;5:803–13.
- [55] Kondo H, Ohyama T, Ohya K, Kasugai S. Temporal changes of mRNA expression of matrix proteins and parathyroid hormone related protein (PTH/PTH-rp) receptor in bone development. *J Bone Miner Res* 1997;12:2089–97.
- [56] Owen TA, Aronow M, Shalhoub V, Barone LM, Wilming L, Tassinari MS, et al. Reciprocal relationships in expression of genes associated with osteoblast proliferation and differentiation during formation of bone extracellular matrix. *J Cell Physiol* 1990;143:420–30.
- [57] Malaval L, Modrowski D, Gupta AK, Aubin JE. Cellular expression of bone related proteins during *in vitro* osteogenesis in rat bone marrow stromal cultures. *J Cell Physiol* 1994;138:555–72.